*Journal of Mechatronics and Robotics*

Original Research Paper

# Prosthetic Knee Mechanism Using a Double Locking System as a Safety Measure

**[1]Eicarl Saynes Vazquez and [2]Esther Lugo González**

*[1]Technological University of Mixteca, Huajuapan de León, Oaxaca, Mexico*
*[2]Institute of Electronics and Mechatronics, Technological University of Mixteca, Huajuapan de León, Oaxaca, Mexico*

*Article history*
Received: 01-12-2023
Revised: 06-12-2023
Accepted: 08-12-2023

Corresponding Authors:
Esther Lugo González
Institute of Electronics and Mechatronics, Technological University of Mixteca, Huajuapan de León, Oaxaca, Mexico
Email: elugog@mixteco.utm.mx

**Abstract:** The design of a four-link knee prosthesis mechanism with two locking systems activated during the flexion/extension phase is presented. The first is geometric, totally mechanical and activated by the user's weight. The second is variable and is activated automatically when walking on irregular or special surfaces is required. The links' dimensions were selected using the differential evolutionary optimization algorithm to follow the trajectory of the poloid generated during human walking. Motion simulation is performed in the Adams view program to validate the trajectory tracking during walking and the operation of the locking systems using the angles obtained from the Opensim program. The plots obtained for the motion in the simulations show that a poloid tracking was generated in 92% as with a healthy knee, particularly in walking and sitting positions. The physical and virtual prototypes are presented and their movement is described when used by a person. During the physical tests, the flexion-extension movement of the mechanism was observed in an approximate range of 0-130°, following the desired trajectory of the poloid. The variable locking system locks the leg in the stay and when seated, allowing free movement during gait.

**Keywords:** Double Locking System, Prosthetic, Knee Mechanisms

## Introduction

Knee prostheses can be monocentric or polycentric and use mechanisms configured according to prescription as well as selection criteria to generate basic flexion and extension movements. Liang *et al.* (2022) describes that these criteria depend on the interaction between the user and the prosthesis, which includes five functional levels ranging from $K_0$ (the patient is unable to move safely and without assistance) to $K_4$ (can move without restriction and tolerate high levels of impact, stress and energy). One of the aims of the design and selection of mechanisms is to avoid joint hyperextension and unwanted movements that could lead to the user becoming unbalanced or falling. To ensure stability in prostheses, braking or locking systems have been developed that are generally activated in situations such as standing, walking up or down stairs and walking on inclined or difficult terrain. The function of the lock is to activate or deactivate the knee joint, allowing or preventing flexion and extension movement (Gue´rinot *et al*., 2004).

The most commonly used manual knee-locking system consists of a lever or latch that is activated by pushing a button or pulling a cord. Liang *et al.* (2022) describe that this type of system is recommended for patients with low mobility ($K_1$) or for geriatric patients. Another is geometry locking, which is a passive method that uses the shape and position of the prosthesis mechanism to prevent knee movement in positions such as hyperextension. Okuda *et al.* (2009) describe a locking mechanism for leg prostheses based on the use of a cam that is automatically activated by knee flexion during the swing phase, stopping the movement of the leg. A locking mechanism that reduces torque during initial knee flexion is described in (Okuda and Yoshiaki, 2013). It consists of a hydraulic damper and a locking system that is activated during the weight-bearing phase. When the user applies weight to the prosthesis, the hydraulic mechanism compresses and the locking system is activated, reducing the torque at the Knee prostheses can be monocentric or polycentric and use mechanisms configured according to prescription as well as selection criteria to generate basic flexion and extension movements. Liang *et al.* (2022)

**DOI: 10.3844/jmrsp.2024.1.10**

describe that these criteria depend on the interaction between the user and the prosthesis, which includes five functional levels ranging from $K_0$ (the patient is unable to move safely and without assistance) to $K_4$ (can move without restriction and tolerate high levels of impact, stress and energy). One of the aims of the design and selection of mechanisms is to avoid joint hyperextension and unwanted movements that could lead to the user becoming unbalanced or falling. To ensure stability in prostheses, braking or locking systems have been developed that are generally activated in situations such as standing, walking up or down stairs and walking on inclined or difficult terrain. The function of the lock is to activate or deactivate the knee joint, allowing or preventing flexion and extension moment of initial knee flexion while improving the stability of the prosthesis. The knee developed by Lu and Chen (2010) features a 6-bar polycentric mechanism with geometric-automatic weight-activated locking. This geometry allows the activation and deactivation of a rigid lock at maximum extension. A passive mechanism for a transfemoral prosthetic knee was Lu designed by Murabayashi *et al.* (2022) to prevent falls during the stance phase of gait. The mechanism blocks flexion while the prosthetic knee is under load and always allows extension by means of a unidirectional clutch. The mechanism's parameters were set with reference to the subject's gait and stance parameters to avoid the inadvertent release of the flexion lock during stance. A review of prosthetic knees from a biomechanical perspective is presented by (Liang *et al.*, 2022) and includes stance phase stability using locking systems, early phase flexion and swing resistance, which directly relate the mechanical mechanisms to perceived gait performance, i.e., fall avoidance, shock absorption and gait symmetry.

In contrast, the automatic locking system typically uses a controller and an electric motor to lock and unlock the prosthesis's movement. Force and position sensors in the devices detect flexion or extension during gait and send a signal to the controller to activate the lock when needed. A hybrid prosthetic knee with active and passive damping modes of operation is currently being developed to achieve energy optimization within the overall system. Escalona and Torrealba (2015), a linear hydraulic actuator with modular response has been designed to actuate and control the prosthetic device, which acts as a variable lock during the patient's gait cycle. Similarly, the research by Wang *et al.* (2020) developed a passive-active hybrid knee with two energy-saving modes of operation, which has an active mode that works with a resistance actuator or a variable lock. Murthy-Arelekatti and Winter (2018), a mechanism is presented that has an automatic initial stance phase lock for stability and a differential friction damping system for stance and roll control. The prototype provides a smooth transition from stance to roll with a timely onset of late stance flexion. Tong and Bhuiyan (2020), an electromagnet-based locking mechanism was developed for a prototype geared knee prosthesis. The electromagnet is controlled by a microcontroller to lock and unlock the knee joint by detecting positional data from a gyroscopic sensor during femoral movement.

Rasheed *et al.* (2023) a review of the state of the art in knee prostheses is presented, with research objectives including stair walking, ramp and uneven surface walking, as well as gait patterns. With respect to the different gait activities, several researchers focused on walking at ground level and stair climbing with improved performance. Most of the prostheses presented used automatic locking for stability.

Overall, the challenge in the locking system is to focus on kinematics and gait analysis using a transfemoral prosthesis for ramp walking to ensure the required symmetrical gait pattern, knee joint angle, torque, power output and impedance control without loading the hip and other healthy limbs. This requires control of the rate of ascent and descent and safety systems such as locks to prevent falls. Based on this, a 4-bar mechanism is proposed, incorporating a geometric lock with a fifth link added to provide a variable.

## Materials and Methods

The design presented is for patients with $K_3$ mobility levels (the patient can move freely on different surfaces and has the ability to walk at different speeds and avoid obstacles in an environment) and is based on a polycentric mechanism.

Kapandji (2010) explains that the knee is a Single Degree-Of-Freedom (SDOF) joint that acts in compression under the action of gravity and this DOF generates the flexion-extension movement that carries out the knee in the sagittal plane in active or passive positions. The polycentric prosthesis consists of a 4-link mechanism connected to an actuation system with a $5^{th}$ link connecting it to the second lock system, as seen in Fig. 1. The DOF is obtained with the Eq. 1:

$$M = 3(N-1) - 2J_1 - J_2 \quad (1)$$

where, $M$ = are the degrees of freedom, $N$ is the number of links, $J_{1\ is}$ the number of kinematic pairs of one degree of freedom and $J_{2\ is}$ the number of kinematic pairs of two degrees of freedom, in agreement with Shigly and Uicker (1988).

For the mechanism in Figs. 1-2 DOF was obtained, so it is a redundant system as there are more degrees of freedom available than necessary to achieve a desired control or motion, this is explained in Arora (2016). To avoid redundancy, the DOF of the 4-link mechanism (passive motion) is used to control the entire system, Fig. 2.

**DOI: 10.3844/jmrsp.2024.1.10**

The second DOF is partially activated when the sensor detects the range of motion of the stay-and-go phase in inclined areas or stairs. The mechanisms can operate independently, allowing the prosthetic leg to function in both passive and active modes.

The 5th link is connected to a semi-threaded shaft through a linear bearing. The first half of the shaft is smooth and the second half is threaded to perform the locking of the mechanism and activate the motor during desired gear positions as seen in Fig. 3. The shaft is joined by a flexible joint with a DC geared motor. The lock is anchored to the $l_1$ link, which represents the system's ground or fixed joint. Finally, there is a linear bearing located on the semi-threaded shaft, which performs a vertical movement along the shaft. The variable describing this motion is denoted by the letter *d*.

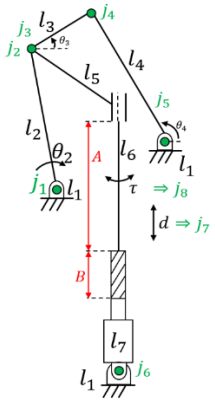


**Fig. 1:** Topological structure of the prosthetic mechanism

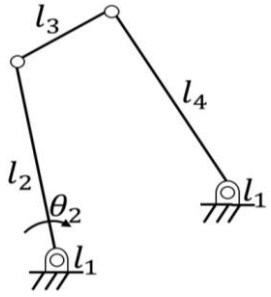


**Fig. 2:** Four-link mechanism

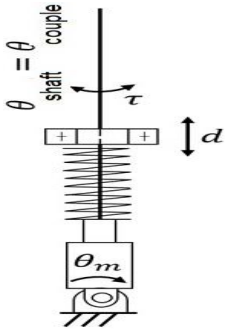


**Fig. 3:** Conceptual design of a second locking

To link the actuator to the coupling and the shaft to generate the motion, Eq. 3 is used:

$$\theta_{\text{motor}} = \theta_{\text{couple}} \tag{2}$$

$$\theta_{\text{couple}} = \theta_{\text{shaft}} \tag{3}$$

where, $\theta_{\text{motor}}$, $\theta_{\text{couple}}$ *y* $\theta_{\text{shaft}}$ are the rotation angles of the motor, flexible coupling and rotation angle of the semi-threaded shaft, respectively.

Equation 4 defines the joint between the flexible coupling and the semi-threaded shaft that transmits the motor motion to the links:

$$\theta_{shaft} = \frac{d}{r} \tag{4}$$

where, *d* is the position of the linear bearing (which can be 0-30 mm) and *r* is the radius of the half-round shaft (3 mm).

### *Mechanism Synthesis*

The Instantaneous Center of Rotation (CIR) is the point around which the leg rotates in flexion and must be located in relation to the patient's anatomy to be functional. Xie *et al.* (2014) mentioned that the degree of similarity between the behavior of a human knee and that of a 4-link knee mechanism is directly proportional to the value of the error of the objective function, i.e., the smaller the error, the closer the CIR of the mechanism to the anatomical CIR of the human leg. For transfemoral prostheses with a 4-link mechanism, this point is generally located at the intersection of the extensions of the anterior and posterior link lines that connect the socket section to the leg in the prosthesis. As the angle of knee flexion increases, the CIR assumes a series of positions that typically follow a trajectory with the leg extended forward and down to the anatomical center of the knee, Fig. 4. This trajectory is known as the poloid and usually has a characteristic C-shape. The poloid provides functionality and meets the needs of the patient. Figure 5 shows the *C* trajectory to form the anatomical poloid of the human knee mentioned in Radcliffe (1994); Salas *et al.* (2021).

The coordinates from Table 1 are then used to trace the poloid, which is used as a reference point to determine the dimensions of the 4-link mechanism used in flexion and extension movements. These data were collected from a patient who is 1.70 m tall, 25 years old and has a physical activity level of $K_3$. Table 2 details the variables and constraints used in the DEA to calculate the dimensions and angles of the mechanism.

**DOI: 10.3844/jmrsp.2024.1.10**

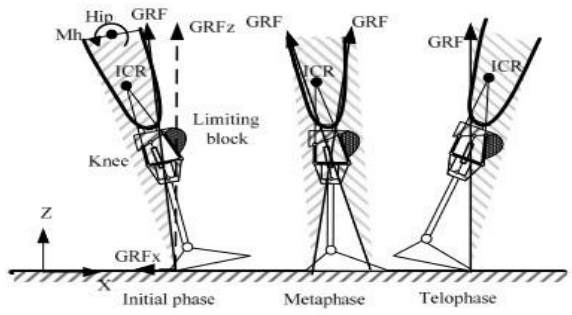


**Fig. 4:** Location of the CIR in the human leg by Xie *et al*. (2014)

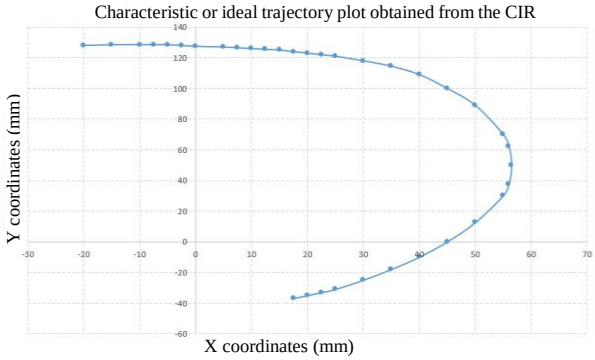


**Fig. 5:** Poloid characteristic by Radcliffe (1994)

**Table 1:** Desired points for the C-shape of a healthy patient

| No. | Xd (mm) | Yd (mm) |
|---|---|---|
| 1 | -19.88 | 721.76 |
| 2 | -9.93 | 724.59 |
| 3 | -1.64 | 725.68 |
| 4 | 06.12 | 725.70 |
| 5 | 18.86 | 723.52 |
| 6 | 29.21 | 719.52 |
| 7 | 37.19 | 714.80 |
| 8 | 44.31 | 709.08 |
| 9 | 50.42 | 702.69 |
| 10 | 57.75 | 692.35 |
| 11 | 63.66 | 680.29 |
| 12 | 67.40 | 668.83 |
| 13 | 70.31 | 651.85 |
| 14 | 70.74 | 637.39 |
| 15 | 68.29 | 615.98 |
| 16 | 60.67 | 590.51 |
| 17 | 56.30 | 580.92 |

**Table 2:** Restrictions for drawing the poloid

| Characteristics | Description |
|---|---|
| Links restriction $r_1$, $r_4$ | (0, 90) in mm |
| $r_2$, $r_3$ | (0, 60) in mm |
| $x_0$ = | 0.0001 in mm |
| $y_0$ = | 500 in mm |
| rcx = | (10, 25) |
| rcy = | (10, 1000) in mm |
| Movement range $\theta_2$ | (0, 110) in grades |
| $\theta_1$ | (0, 50) in grades |
| Crossover probability | 0.6 |
| Mutation probability | 0.4 |
| Precision | 4 digits after the period |
| Maximum generations | 1000 |

For the synthesis of 4-link mechanisms, the freudenstain equation is used and solved by optimization with a Differential Evolutionary Algorithm (DEA). Optimization is used to define the best system configuration with the aim of maximizing efficiency and minimizing error in trajectory tracking. The development for poloid tracking and optimization of the 4-link mechanism is presented in Saynes-Vazquez and Lugo-González (2022). This begins with the approach of (Eqs. 5-7) to obtain the angles of motion and the dimensions of the links:

$$\cos(\theta_3) = \frac{l_3^2 + l_2^2 - l_4^2 - l_1^2 + 2l_3 l_2 \cos(\theta_4)}{2l_3 l_2} \tag{5}$$

$$\cos(\theta_4) = \frac{l_4^2 + l_1^2 - l_3^2 - l_2^2 + 2l_4 l_1 \cos(\theta_2)}{2l_4 l_1} \tag{6}$$

$$\cos(\theta_2) = \frac{l_3^2 + l_2^2 - l_4^2 - l_1^2 + 2l_3 l_2 \cos(\theta_3)}{2l_3 l_2} \tag{7}$$

For the optimization, the reference path that the work C-shape will follow is used. In this case, they are the coordinates of Table 1. The objective function used for the optimization is defined as (Eq. 8):

$$F(x) = \sum_{i=1}^{N} \left[ \left( X_i^d - X_i^c \right)^2 + \left( Y_i^d - Y_i^c \right)^2 \right] \tag{8}$$

where, the first term defines the position error as the squared difference of the Euclidean distances between $X_{\text{desired}}$ and $X_{\text{calculated}}$ of the tracking C-shape. The second term performs the same calculation but for the distances in *Y*. *N* represents the number of points to synthesize.

Figure 6 shows a comparison between the desired poloid and the one obtained. It can be seen that the start of the two curves coincides approximately at (-20, 128) and that the orange curve, for the last 5 points of the path marked by the blue curve, approaches smoothly, i.e., without any disturbances. It has thus been verified that the geometrical arrangement of the mechanism's bars produces a poloid that is 92% similar to that established for a healthy knee during walking and sitting, as mentioned in Xie *et al*. (2014).

Finally, the values for the mechanism's links are shown in Table 3.

## *Locking System*

The mechanical design of the polycentric prosthesis takes into account a manual locking mechanism activated by the user. This is geometric and acts during the maximum extension of the prosthetic leg i.e., when the patient is in the stance phase and the total weight of the patient is on the load line of the leg. Figure 7, the red boxes with dashed lines show the mechanism for geometric locking between the white link (bed of the 4-link mechanism) and the yellow link (crank). The flexion or extension movement is performed in the sagittal plane with a clockwise rotation.

**DOI: 10.3844/jmrsp.2024.1.10**

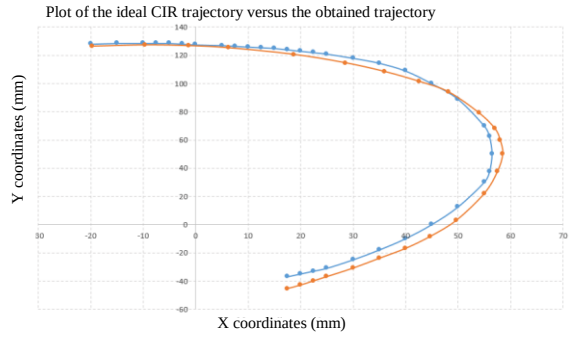


**Fig. 6:** Characteristic poloid vs obtained

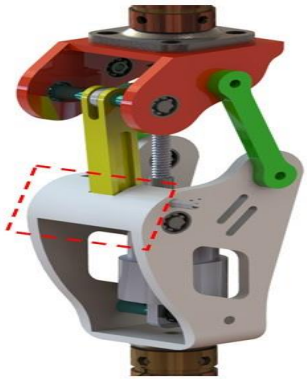

**Fig. 7:** Primary geometric locking design

**Table 3:** Links' dimensions and angles of the polycentric mechanism

| Variable | Value |
|---|---|
| $L_1$ | 58.75 in mm |
| $L_2$ | 89.53 in mm |
| $L_3$ | 35.49 in mm |
| $L_4$ | 78.92 in mm |
| $L_5$ | in mm |
| $L_6$ | in mm |
| $L_7$ | in mm |
| θ1 | 29.93° |
| θ2 | 64.96° |
| θ3 | 24.21° |
| θ4 | 79.45° |

The second locking mechanism is defined as a variable and is the partial locking of the modified worm screw and trapezoidal nut by linear movements during intervals defined by the flexion-extension angles of the prosthetic leg. During the first 35° of motion, the trapezoidal nut slides freely on the smooth surface of the screw due to the passive movements of the mechanism. For angles greater than or equal to 36° and up to 90° from the load line of the prosthetic leg, the nut continues its linear movement, but now on the threaded surface. The change from one surface to the other, together with a motor equipped with a classic Proportional Integral Differential control (PID), provides stability during this second range of movement in the desired positions, as well as partial locking and control of the polycentric knee. Figure 8 shows the isometric view of the mechanism of the polycentric prosthesis, including the second locking system.

## *Virtual Prototype*

The Opensim software was used to generate the trajectory that the prosthesis mechanism follows in Adamsview to visualize the movement and check that there are no singularities. Opensim is an open-access tool for modeling and simulating the movement of the human body (Uchida *et al*., 2020). Furthermore, Adamsview is a computational software focused on the dynamic analysis of multi-body systems and its main objective is to solve non-linear problems. It facilitates the analysis of the dynamics of moving parts, as well as the loads and forces distributed throughout mechanical systems (McConville, 2015).

Two movements of the prototype were analyzed: The sitting position and stair climbing. For demonstration purposes, the prosthetic leg was modeled as a simple pendulum, considering for the unipod and sitting positions zero friction, active gravity of 9.81 m/s$^2$ in the downward *y* direction, 2 seconds as the total simulation time, non-contact elements and oscillatory type rotary motion at 1 Hz frequency and 90° amplitude.

Figure 9 shows the leg in a unipodal position, in contact with the ground (green). To start walking, an oscillating motion is defined from -90 to 0°, starting from the load line of the leg, to simulate the sitting position. In this test, the links, post and foot remain fixed, while links 2-4, together with the socket, are mobile.

**Fig. 8:** Different views of polycentric prosthesis

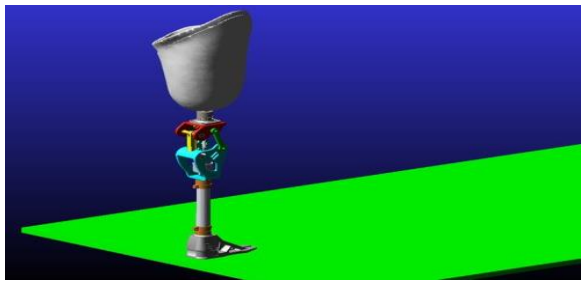

**Fig. 9:** Prosthetic prototype: Simulation in Adams's view

**DOI: 10.3844/jmrsp.2024.1.10**

For sitting, the range of motion was 90-180° from the load line of the prosthetic leg, Fig. 10.

Figure 11, a unipodal posture is shown to bring the prosthetic leg to different positions in a range of motion from 0-120°.

The input value is $\theta_1$ and can be varied between 26° and 29.3° to better follow the poloid according to the patient's characteristics. Figure 12, the simulation allows the comparison of the trajectory obtained from the operating point *C* with the desired trajectory. The black dashed line represents the reference or desired curve, the orange solid line corresponds to the trajectory obtained with an angle $\theta_1$ of 26°, while the blue line is a modification of the entry angle $\theta_1$ of 29.3°.

For the second analysis, a movement was simulated by using subroutines for the leg to climb stairs. As the movement for descent is different from that for the ascent, the same subroutines are used in the opposite direction for descent. Contact forces are simulated in Adamsview, both between the foot and the floor and with the double locking system.

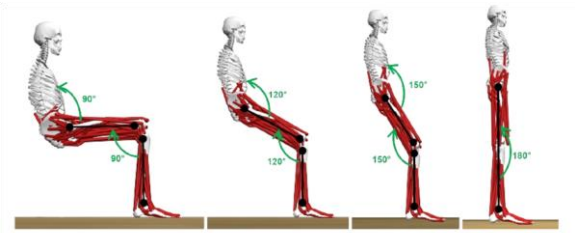


(a)

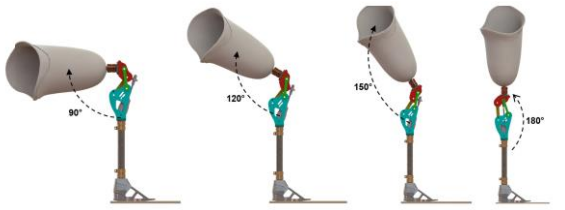


(b)

**Fig. 10:** Movement phases for sitting and standing; (a) Opensim dummy in sitting position; (b) Mechanical design

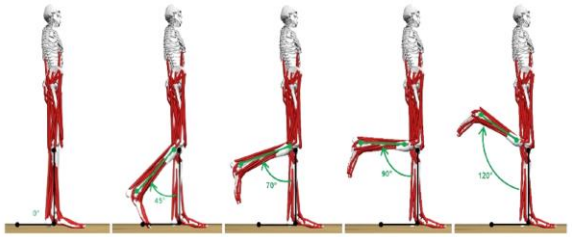

(a)

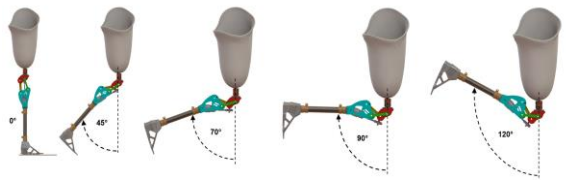


(b)

**Fig. 11:** Unipodal position: Phases of the flexion movement with; (a) Opensim dummy during flexion movements; (b) Mechanical design

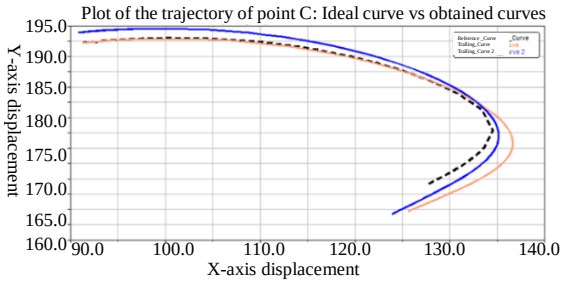


**Fig. 12:** Trajectory of poloid characteristic versus obtained

Figure 13 shows that it is necessary to move the knee and hip in order to walk. To simulate this movement, a rotating joint is placed in the socket to allow simultaneous rotation and translation, simulating the movement of the hip during walking. The graph in Fig. 14 shows the path that the prosthetic leg takes in a time of 2.4 sec to go up and down the three steps that have been placed. The (x, y) coordinate graph takes this shape due to the up-and-down movement of the leg as it walks on the steps.

Regarding the locks, it was observed that the first one kept the device in a fixed position, considering the geometry of the first link. As for the second, the variable lock, it developed a linear movement during the first phase of the trajectory, at the start of the foot and was locked when the section of the axis that has the rope in the thread finishes the extension to have the sitting position. This lock is deactivated only when the motor is activated.

## *Physical Prototype*

Some of the materials chosen for the design of the virtual prototype are aluminum, steel alloys, ABS and PLA. The ABS and PLA were used for some parts that were not exposed to high loads.

During the physical tests, the flexion-extension movement of the mechanism was observed in an approximate range of 0-130°, following the desired trajectory of the operating C-shape. The proposed variable locking system interrupted the movement of the leg in positions such as going up and down stairs, making walking much slower but safer.

**DOI: 10.3844/jmrsp.2024.1.10**

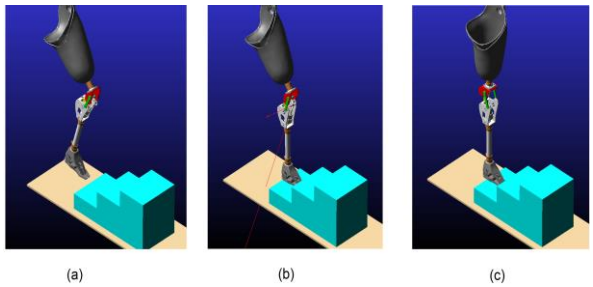


**Fig. 13:** Step gait simulation in Adams view; (a) Average swing; (b) Support and; (c) Final position

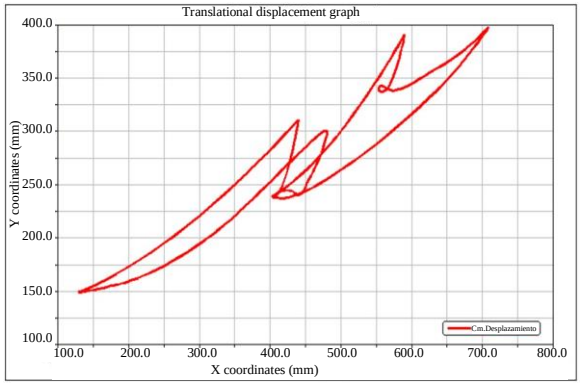


**Fig. 14:** Complete walking path on steps at Adams view

Figure 15 shows the primary lock formed by links 1 (orange) and 2 (black). The first lock is based on the mechanism's geometry, while the second is a variable system. The first lock provides safety and stability for the patient during full extension of the prosthetic leg, both when standing and in the initial and final phases of the gait cycle. Link 2 has a natural counterclockwise restriction, allowing only clockwise movement.

Images of the final prototype, which comprises the mechanical and electronic systems, are shown in Fig. 16. Sections (a-b) show the position of the prosthetic leg at maximum flexion, which is approximately 130°.

To provide the mechanism movement, a basic electronic system was implemented, as seen in Fig. 17. This is controlled by an Arduino microcontroller, which uses PID control to manipulate a gear motor with an incremental encoder connected to an H-bridge driver. This device manipulates the rotation of the motor in clockwise and counterclockwise directions. A classic PID controller was implemented for control. The aim was to control the desired positions of the actuator with the MP6050 sensor. To manipulate the low speed and high torque, a 12 V DC, 120 mA geared motor was used, which has a speed of 20 rpm without load, a reduction ratio of 1:506 and 11 pulses per second. An oscillation test was carried out using the prototype as a simple pendulum model and two control strategies (P and PID) were implemented to observe the control response to large disturbances. A controlled oscillation test and flexion-extension motions were performed to determine the control response and settling time at the reference value.

**Fig. 15:** Primary lock system


**Fig. 16:** Final physical prototype; (a) Lateral view and (b) View of the sitting position, with maximum flexion at 130°

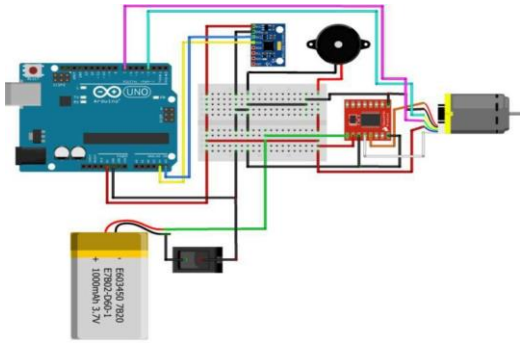

**Fig. 17:** Electronic and control system

**DOI: 10.3844/jmrsp.2024.1.10**

## Results and Discussion

The tests carried out were:

Monitoring of the poloid: This consisted of observing that the curve obtained tried to match the desired one in the simulation carried out in the MATLAB program. This graphical information is validated by minimizing the error obtained at the end of the monitoring. As can be seen in Figure 11, the developed mechanism follows the desired trajectory with an error of 8%, which according to Lu and Chen (2010), is within acceptable limits, provided that the starting point of the trajectory is at (-20,128) mm and the end points of the curve are smooth and correspond to the anatomical CIR trajectory.

Stability: The stability of the prosthesis was visually verified when the user climbed and descended stairs and walked on tiled floors and on cement floors. It was found that the system functioned correctly in terms of movement, but that the PLA materials were not strong enough. Professional prostheses should be made in aluminum or carbon fiber, as mentioned in Tibisay *et al.* (2014).

Static load: The user's 65 kg load was applied to different positions and angles of the prosthesis to verify its ability to support the load. It was found that some parts needed to be replaced with more resistant materials such as aluminum.

Dynamic loading: This consisted of applying dynamic loads to different positions and angles of the prosthesis to verify its ability to withstand moving loads. It was observed that it was necessary to replace some parts with more resistant materials such as aluminum.

Control system: It was verified that the response time of the control system was sufficient to follow the reference when activated in situations such as climbing stairs or ramps. A controlled oscillation test and flexion-extension movements were performed to determine the control response and the settling time at the reference value. Figure 18 it can be seen that the blue signal represents the reference or setpoint and the green signal represents the real-time controller value. The controller follows the setpoint during the simulation time. Although the noise in the signal has not been eliminated, it can be seen that the controller allows flexion extension, oscillation and sitting and walking movements for the range of angles defined.

Tests were carried out on a 65 kg, 21-year-old user with $K_3$ activity, Fig. 19.

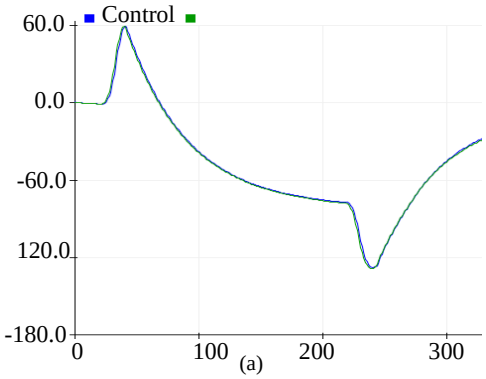


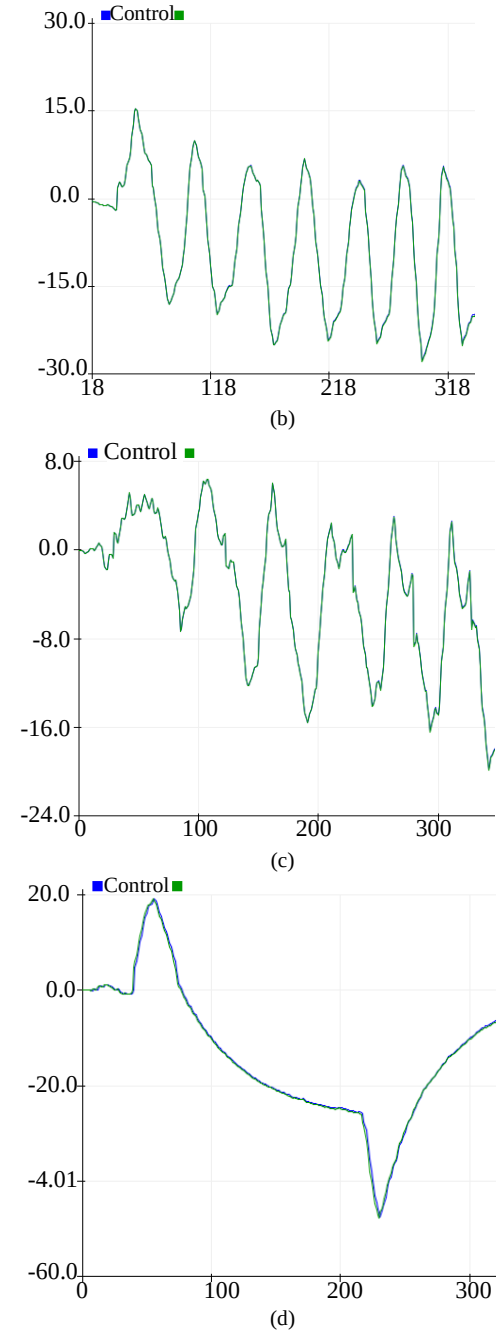


**Fig. 18:** Control system results; (a) Oscillation; (b) Flexo-extension; (c) Climbing and (d) Sitting


**Fig. 19:** Physical tests of the mechanism; (a) Back view and (b) Front view

## Conclusion

A double locking mechanism can improve the stability of a prosthesis during stance and in situations such as climbing stairs or slopes. By providing an additional variable lock, greater control is achieved and unwanted movement is prevented. The active mode of operation with additional locking allows the prototype to adapt and respond to the user's actions, providing greater control when climbing stairs or slopes and adapting to individual needs. Virtual and physical tests were carried out. During the physical tests, the flexion-extension movement of the mechanism was observed in an approximate range of 0-130°, following the desired trajectory of the operating C-shape. The variable locking system locks the leg in the stay and when sitting, allowing free movement when walking.

## Acknowledgment

The authors would like to thank the Technological University of Mixteca and the National Council of Humanities, Sciences and Technologies; abbreviated Conahcyt) for their support.

## Funding Information

The authors have not received any financial support or funding to report.

## Author's Contributions

**Esther Lugo:** Contributes to the conception, design, analysis, and interpretation of data. Drafts the article or critically reviews it for significant intellectual content. Provides final approval of the version to be submitted and any revised versions.

**Eicarl Saynes:** Contributes to the conception, design, acquisition of data, and analysis and interpretation of data. Reviews the significant intellectual content. Gives final approval of the version to be submitted and any revised versions.

## Ethics

This article is original and contains unpublished material. The corresponding author confirms that the second author has read and approved the manuscript. The authors declare that there are no ethical issues and no conflict of interest that may arise after the publication of this manuscript.

## References

Arora, J. S. (2016). Introduction to optimum design. *USA: Academic Press*. (*4*)(1), 1103-1111. https://doi.org/10.1016/C2013-0-15344-5

Escalona, J. & Torrealba R. R. (2015). Design of linear hydraulic actuator of variable response for intelligent knee prosthesis. Memorias del V Congreso Venezolano de Bioingeniería. *Universidad de Los Andes*. *18*-21.

Gue´rinot, A. E., Magleby, S. P., & Howell, L. L. (2004). Preliminary design concepts for compliant mechanism prosthetic knee joints. In *International Design Engineering Technical Conferences and Computers and Information in Engineering Conference* (Vol. 46954, pp. 1103-1111). https://doi.org/10.1115/DETC2004-57416

Kapandji, A. I. (2010). Fisiologia articular tomo II2018. Design, development and testing of a lightweight hybrid robotic knee prosthesis. *The International Journal of Robotics Research*, *37*(8), 953-976. https://doi.org/10.1177/0278364918785993

Liang, W., Qian, Z., Chen, W., Song, H., Cao, Y., Wei, G., ... & Ren, L. (2022). Mechanisms and component design of prosthetic knees: A review from a biomechanical function perspective. *Frontiers in Bioengineering and Biotechnology*, *10*, 950110. https://doi.org/10.3389/fbioe.2022.950110

Lu, J., & Chen, Y. (2010, December). Topology optimization of a prosthetic knee joint component. In *2010 International Conference on Manufacturing Automation* (94-98). IEEE. https://doi.org/10.1109/ICMA.2010.52

McConville, J. B. (2015). *Introduction to Mechanical System Simulation Using Adams*. SDC publications. ISBN-10: 9781585039883.

Murabayashi, M., Mitani, T., & Inoue, K. (2022). Development and evaluation of a passive mechanism for a transfemoral prosthetic knee that prevents falls during running stance. *Prosthesis*, *4*(2), 172-183. https://doi.org/10.3390/prosthesis4020018

Murthy-Arelekatti, V. N., & Winter, A. G. (2018). Design and preliminary field validation of a fully passive prosthetic knee mechanism for users with transfemoral amputation in India. *Journal of Mechanisms and Robotics*, *10*(3), 031007. https://doi.org/10.1115/1.4039222

Okuda, M., & Nakaya, Y. (2013). *U.S. Patent No. 8,529,634*. Washington, DC: U.S. *Patent and Trademark Office*. https://patents.google.com/patent/US8529634B2/en

Okuda, M., Imakita, T., Fukui, A., & Nakaya, Y. (2009). *U.S. Patent No. 7,588,604*. Washington, DC: U.S. Patent and Trademark Office. https://patents.google.com/patent/US7588604B2/en

Radcliffe, C. W. (1994). Four-bar linkage prosthetic knee mechanisms: Kinematics, alignment and prescription criteria. *Prosthetics and Orthotics International*, *18*(3), 159-173. https://doi.org/10.3109/03093649409164401

Rasheed, F., Martin, S., & Tse, K. M. (2023). Design, kinematics and gait analysis, of prosthetic knee joints: A systematic review. *Bioengineering*, *10*(7), 773. https://doi.org/10.3390/bioengineering10070773

Salas, P., Vergara, M., & Provenzano, S. (2021). Prótesis de rodilla: Fundamentos teóricos y técnicas computacionales para su diseño knee prosthesis: theoretical foundations and computational techniques applied to its design. *Revista Ciencia e Ingeniería*, *42*(1). ISSN-10: 1316-7081.

Saynes-Vazquez, E., & Lugo-González, E. (2022). Optimización de mecanismos planos de 4 y 6 eslabones para el desarrollo de un prototipo de prótesis transfemoral. *Res. Comput. Sci.*, *151*(6), 47-62. ISSN-10: 1870-4069.

Tibisay, A. B., Muller-K. C. & Torrealba, R. R. (2014). Structural rectification in the design of polycentric knee prosthesis using finite elements. In Proceedings of XII congreso internacional de métodos numéricos en ingeniería y ciencias aplicadas. *CIMENICS 2014*. ISBN-10: 9789807161046.

Tong, C. X., & Bhuiyan, M. S. H. (2020). An investigation into a locking mechanism designed for a gear-based knee joint prosthesis. *Cogent Engineering*, *7*(1), 1738186. https://doi.org/10.1080/23311916.2020.1738186

Uchida, T. K., & Delp, S. L. (2021). *Biomechanics of Movement: The Science of Sports, Robotics and Rehabilitation*. Mit Press. ISBN-10: 9780262044202.

Wang, X., Meng, Q., Zhang, Z., Sun, J., Yang, J., & Yu, H. (2020). Design and evaluation of a hybrid passive-active knee prosthesis on energy consumption. *Mechanical Sciences*, *11*(2), 425-436. https://doi.org/10.5194/ms-11-425-2020

Xie, H., Wang, S., & Li, F. (2014). Knee joint optimization design of intelligent bionic leg based on genetic algorithm. *International Journal Bioautomation*, *18*(3), 195. https://biomed.bas.bg/bioautomation/2014/vol_18.3/files/18.3_03.pdf